

Adaptive potential in the face of a transmissible cancer in Tasmanian devils

Kasha Strickland¹  | Menna E. Jones²  | Andrew Storfer³ | Rodrigo K. Hamede²  |
 Paul A. Hohenlohe⁴  | Mark J. Margres⁵  | Hamish I. McCallum⁶  |
 Sebastien Comte⁷  | Shelly Lachish⁸ | Loeske E. B. Kruuk¹ 

¹School of Biological Sciences, Institute of Ecology and Evolution, University of Edinburgh, Edinburgh, UK

²School of Natural Sciences, University of Tasmania, Hobart, Tasmania, Australia

³School of Biological Sciences, Washington State University, Pullman, Washington, USA

⁴Department of Biological Sciences, University of Idaho, Moscow, Idaho, USA

⁵Department of Integrative Biology, University of South Florida, Tampa, Florida, USA

⁶Environmental Futures Research Institute, Griffith University, Nathan, Queensland, Australia

⁷Vertebrate Pest Research Unit, NSW Department of Primary Industries, Orange, New South Wales, Australia

⁸Public Health Intelligence Branch, Queensland Public Health and Scientific Services Division, Queensland Health, Herston, Queensland, Australia

Correspondence

Kasha Strickland, School of Biological Sciences, Institute of Ecology and Evolution, University of Edinburgh, Edinburgh, UK.
 Email: kasha.strickland@ed.ac.uk

Funding information

NSF Division of Environmental Biology, Grant/Award Number: DEB-1316549 and DEB-2027446; Common Fund; European Research Council, Grant/Award Number: 101020503; Australian Research Council, Grant/Award Number: DP110102656, LP0989613, LP0561120, A00000162 and FT100100031; The Royal Society, Grant/Award Number: RSRP\R1\211017; NIH, Grant/Award Number: R01-GM12653

Handling Editor: Sebastien Calvignac-Spencer

Abstract

Emerging infectious diseases (EIDs) not only cause catastrophic declines in wildlife populations but also generate selective pressures that may result in rapid evolutionary responses. One such EID is devil facial tumour disease (DFTD) in the Tasmanian devil. DFTD is almost always fatal and has reduced the average lifespan of individuals by around 2 years, likely causing strong selection for traits that reduce susceptibility to the disease, but population decline has also left Tasmanian devils vulnerable to inbreeding depression. We analysed 22 years of data from an ongoing study of a population of Tasmanian devils on Freycinet Peninsula, Tasmania, to (1) identify whether DFTD may be causing selection on body size, by estimating phenotypic and genetic correlations between DFTD and size traits, (2) estimate the additive genetic variance of susceptibility to DFTD, and (3) investigate whether size traits or susceptibility to DFTD were under inbreeding depression. We found a positive phenotypic relationship between head width and susceptibility to DFTD, but this was not underpinned by a genetic correlation. Conversely, we found a negative phenotypic relationship between body weight and susceptibility to DFTD, and there was evidence for a negative genetic correlation between susceptibility to DFTD and body weight. There was additive genetic variance in susceptibility to DFTD, head width and body weight, but there was no evidence for inbreeding depression in any of these traits. These results suggest that Tasmanian devils have the potential to respond adaptively to DFTD, although the realised evolutionary response will critically further depend on the evolution of DFTD itself.

KEYWORDS

adaptive potential, inbreeding depression, quantitative genetics, selection differential, transmissible cancer, wildlife disease

This is an open access article under the terms of the [Creative Commons Attribution](https://creativecommons.org/licenses/by/4.0/) License, which permits use, distribution and reproduction in any medium, provided the original work is properly cited.

© 2024 The Author(s). *Molecular Ecology* published by John Wiley & Sons Ltd.

1 | INTRODUCTION

Emerging infectious diseases (EIDs) are often critical drivers of population and evolutionary dynamics in their host species (Daszak et al., 2000; Schrag & Wiener, 1995). In particular, EIDs can induce rapid evolutionary responses in traits that determine hosts' exposure to pathogens (Herrera & Nunn, 2019), pathogen load (Rigby et al., 2002) and/or the costs of infection (Medzhitov et al., 2012), especially in cases where EIDs impact fertility or cause rapid mortality (Altizer et al., 2003; Cunningham et al., 2021). However, while the ecological impacts of EIDs in natural populations are widely reported, including rapid population decline and species range contractions (Fisher & Garner, 2020; Hoffmann, Zimmermann et al., 2017; Hoyt et al., 2021), empirical evidence for evolutionary consequences of the emergence of infectious diseases in wild populations has been more limited likely due to a lack of appropriate individual-based data (but see, e.g., Bonneaud et al., 2019).

Emerging infectious diseases should select for traits which improve host immune defences (Hayward et al., 2014; Rarberg & Stjernman, 2003), but an adaptive evolutionary response in the susceptibility to disease is dependent on there being standing genetic variation in immune-related traits (Hoffmann, Sgrò & Kristensen, 2017). In wild populations, genetic variation in traits can be estimated by combining individual-level phenotypic data with either a pedigree or genomic relatedness data (Wilson et al., 2010), and although these data are hard to collect in natural populations, some recent studies have used data from long-term field projects to estimate genetic variance in susceptibility to disease. These studies have reported a range of estimates of genetic variance from a heritability of 0.12 for *Mycobacterium bovis* infection in European badgers (Marjamäki et al., 2021) and 0.13 for *Chlamydia pecorum* infection in koalas (Cristescu et al., 2022) to a relatively high heritability of 0.55 for *Mycoplasma ovipneumoniae* infection in bighorn sheep (Martin et al., 2021). In addition to immune traits, selection caused by EIDs could also impact traits that are genetically correlated with individuals' susceptibility to the disease. Body size, for instance, is an important fitness-related trait that often shapes individual variation in life-history traits (Healy et al., 2019) and may be correlated with disease traits as a result of its relationship with immunocompetence or trade-offs caused by differential allocation of resources (Coltman et al., 2001; Gleeson et al., 2005; Silk & Hodgson, 2021; Valenzuela-Sánchez et al., 2021).

While EIDs may induce selection for immune traits and those genetically correlated with them, population declines following the emergence of disease can also cause a rapid decline in genetic diversity concurrent with an increase in inbreeding (Hedrick & Kalinowski, 2000). Increased inbreeding causes increased genome-wide homozygosity and, where this directly impacts fitness, will result in inbreeding depression (i.e., reduced fitness caused by inbreeding) (O'Grady et al., 2006). Due to the tight association between disease traits and fitness components

(i.e., survival and/or reproduction), immune traits are likely to be depressed under increased inbreeding (Spielman et al., 2004), which has been documented in a number of wild animals (e.g., Reid et al., 2003; Ross-Gillespie et al., 2007; Trinkel et al., 2011). When assessing the evolutionary impact of EIDs in declining populations, it is therefore necessary to test for inbreeding depression in immune-related traits.

An EID currently imposing extreme selection in a wild animal population is the transmissible cancer, devil facial tumour disease (DFTD), in Tasmanian Devils (*Sarcophilus harrisii*). Tasmanian devils are the largest extant carnivorous marsupial and are endemic to the island of Tasmania, Australia. DFTD is a transmissible cancer that originated in a single Schwann cell in the 1980s (Murchison et al., 2010; Patton et al., 2020) and has since spread across almost the entirety of the species' range (Cunningham et al., 2021). Tumour cells are transmitted between hosts by allograft often during aggressive interactions in the mating season or in competitive carrion feeding interactions when biting occurs (Hamede et al., 2013). With very few exceptions (Pye et al., 2016), DFTD evades an immune response, becomes malignant and causes mortality within 6–9 months of symptom onset (McCallum, 2008). As a result, DFTD has caused local population declines of over 80% (Cunningham et al., 2021; McCallum et al., 2007). Given the near 100% mortality associated with DFTD once infected, as well as fewer offspring associated with shorter lifespans caused by DFTD (Lachish et al., 2009), it is likely that the emergence of the disease has generated strong selection for traits that reduce the probability of infection (hereafter, susceptibility to disease), and hence also on any genetically correlated traits. Accordingly, several studies have provided evidence for phenotypic and genomic changes in devil populations since the arrival of DFTD. First, allele frequencies at some immune-function genes have changed since DFTD emerged, indicating that there might be contemporary selection on immunity (Epstein et al., 2016; Stahlke et al., 2021). Second, the rate of females breeding at 1 year's old increased sharply after DFTD was first detected (Jones et al., 2008), and while reduced food competition associated with population decline may cause increased growth rates (and hence higher chances of precocial breeding), selection may have played a role in the shift to precocial breeding (Lachish et al., 2009). Further, a genome-wide association study has suggested that susceptibility to DFTD may be linked to certain regions of the genome (Margres et al., 2018). However, in this study, confidence in the heritability estimates for susceptibility to DFTD estimated across multiple genetically differentiated populations (using case-control data) was very low (i.e., posteriors ranged essentially from zero to one), resulting in a high degree of uncertainty as to whether there may be a genetic variance associated with the trait. Finally, selection by DFTD appears to swamp out selection by local abiotic factors (Fraik et al., 2020), indicating the ecological importance of the disease.

In this study, we applied quantitative genetic analyses to data collected from a closely monitored wild population of Tasmanian devils on Freycinet Peninsula, on the east coast of Tasmania, to estimate the potential for an evolutionary response following the

emergence of DFTD. In particular, we used genomic relatedness data to estimate the extent of genetic variation and/or inbreeding depression in susceptibility to DFTD, as well as to measure the phenotypic and genetic correlations between susceptibility to DFTD and body size. In Tasmanian devils, skeletal body size may be subject to disease-induced selection as skeletal size commonly predicts social dominance, which in turn increases the frequency of the types of social interaction which result in disease transmission (Hamede et al., 2008, 2009; Hamilton et al., 2020). Furthermore, body weight may be subject to selection as it is commonly a predictor of immunocompetence across many taxa (Coltman et al., 2001; Gleeson et al., 2005). Assuming individuals have equal probability of exposure [e.g., is present in all spatial locations (Cunningham et al., 2021)], susceptibility to DFTD should act as a proxy for individual fitness (i.e., survival and reproductive success) because mortality post-infection with DFTD is almost 100% and a shorter lifespan associated with contracting the disease reduces the total number of offspring an individual has (Lachish et al., 2007, 2009). Therefore, the phenotypic and genetic correlations of individuals' DFTD infection status with size traits should approximate the predicted change in size traits resulting from selection induced by DFTD (Price, 1970; Robertson & Lewontin, 1968). Under these general predictions, we specifically aim to (1) infer disease-induced selection by estimating phenotypic and genetic correlations between susceptibility to DFTD and size, (2) estimate genetic variation in susceptibility to DFTD and (3) test for inbreeding depression by estimating the relationship between inbreeding and susceptibility to DFTD or size traits (i.e., head width and body weight).

2 | MATERIALS AND METHODS

2.1 | Tasmanian devil study site, trapping and phenotypic data

We used data collected between January 1999 and May 2021 during an ongoing mark-recapture study of Tasmanian devils on the Freycinet Peninsula, Tasmania, Australia. DFTD first appeared at this site in 2001, resulting in 2-year data pre-disease emergence followed by 20 years of data after disease arrival, as the population descended into long-term decline. Tasmanian devils were trapped across the entire 160 km² peninsula up to four times a year using custom-built baited traps (Lachish et al., 2007), with trapping periods timed to coincide with key stages in the breeding cycle: autumn (April/May), small pouch young; winter (July/August), large pouch young; spring (October/November), females lactating with young in dens; summer (January/February), dependent young emerging from dens. At their first capture, devils were sexed, individually tagged with an ear tattoo (from 1999 to 2004) or a microchip (after 2004) and a 3-mm biopsy sample of tissue taken from the outer edge of the ear for genetic analysis (see below). At first capture and then at all subsequent recaptures their age, head width (in mm) and body weight (in kg) were recorded as described in Lachish et al. (2007). Head width

is measured across the bony jugal arches of the skull covered by skin with no muscle or fat deposits and is therefore a precise measure of skeletal body size. Pouch young of trapped females were sexed and measured, but ear tissue samples were generally not taken because this would result in larger biopsy scars as the individual grew to adult size. A small number of matched pouch young and mothers were sampled between 2000 and 2003, with 2 mm biopsy tissue samples taken from $N=64$ pouch young of $N=27$ mothers and subsequently sequenced (see below). This allowed us to use these known relatives to assess accuracy and precision of genetic relatedness estimation (see below for details). Individuals were aged using a combination of head width, molar eruption, molar tooth wear and canine over-eruption (Jones, 2023), and given a birthdate of April 1st for a given year, as per Lachish et al. (2007). This method of aging is accurate up to 2 years of age, but most individuals were first trapped as juveniles and were therefore of precisely known age. Disease status (presence/absence) was determined for each capture by visual inspection for tumours and/or histopathological examination of tumour biopsies (Hamede et al., 2015; Hawkins et al., 2006). This measure of disease status measures infection status once an individual has become symptomatic which is, on average, 60 days post infection (Wells et al., 2017), and all individuals that are infected with DFTD become symptomatic after this period (Hawkins et al., 2006). The long-term study is conducted with permission and permits granted by the Tasmanian government and with animal ethics approval from the University of Tasmania.

The total number of capture records across the 22 years was 2156 across 972 individuals, giving an average number of captures per individual of 2.31 (min = 1, max = 11), and DFTD was confirmed in 10% of these captures with 17% of individuals caught with DFTD at least once. Average age at capture was 22 months (interquartile range = 16–31 months), and average age at capture with infection was 27 months. The analyses presented in this study used two different subsets of the full dataset collected during the long-term project. For both datasets, we only included observations from individuals that were at least 14 months old. This was done (1) to minimise conflation of age and size measurements, and (2) because this is the age at which female devils can be sexually mature such that biting interactions begin and they can thus be at risk of contracting DFTD (Jones et al., 2008). The first dataset was used for analyses of phenotypic relationships (see 2.5 Statistical analysis section). After removing observations of individuals younger than 14 months and those where there were missing data, this dataset consisted of 1550 recaptures of 729 individuals (hereafter “phenotypic dataset”; 354 males and 375 females). The second subset included captures of individuals for which we also had genetic data in addition to phenotypic data. Genetic data (described below) were used to estimate genetic relatedness and inbreeding coefficients needed for quantitative genetic analyses to estimate additive genetic variance and inbreeding depression, as well as genetic covariances between traits (see 2.5 Statistical analysis section). This dataset was comprised of 498 observations of 243 individuals (hereafter “genetic dataset”; 121 males and 122 females).

2.2 | DNA extraction and genotyping

We extracted DNA from tissue samples and conducted genotyping as previously described elsewhere (Epstein et al., 2016; Margres et al., 2018). Briefly, single-nucleotide polymorphism (SNP) genotyping was achieved via single-digest *RADcapture* ("Rapture" (Ali et al., 2016)) of DNA extracted from tissue. The first round of sequencing that was conducted with this population resulted in data that were of low sequencing depth. As a result, most samples were subsequently re-sequenced in another run to achieve deeper sequencing depth, thereby improving genotyping accuracy. This resulted in an average sequencing depth per individual sample of 6X (averaged across all loci, min=4.4, max=19.3). Reads generated from these replicate runs of the same individuals were merged after aligning to the reference genome, and SNP calling was conducted using the merged "bam" files using the stacks pipeline as in Stahlke et al. (2021). All raw reads from sequencing were first aligned to the *S. harrisii* reference genome (Murchison et al., 2012). PCR duplicates were then removed, and SNPs were discovered and called using *gstacks* (Catchen et al., 2013). The function *populations* was then used to filter SNPs to keep one random SNP per RAD locus and per 10kb window, exclude SNPs with a minor allele frequency (MAF) below 1%, remove individuals with more than 70% missing data and remove SNPs that were present in <50% of the samples. We then further filtered genotype calls with a read depth of <4 in order to increase genotyping accuracy before reapplying the filtering parameters explained above. This resulted in a total of 2105 SNPs genotyped in a total of 584 individuals.

2.3 | Genomic relatedness estimates

Quantitative genetic analyses used to partition phenotypic variance into additive genetic and environmental effects are often achieved by estimating relatedness via a pedigree (Kruuk, 2004; Wilson et al., 2010), which can be based on field observations and/or constructed using genetic marker data. Unfortunately, irrespective of the SNP filtering parameters we used, we were unable to determine sufficient numbers of parentage assignments for a pedigree that could be used for analyses: of 651 individuals, we were only able to assign maternities to 160 and paternities to 175 ($N=83$ individuals with both parents assigned). We were also only able to match 40 of 64 known mother-offspring (pouch young) relationships, with the remaining 24 either not assigned to a mother or mismatched. However, estimating relatedness via a genomic relatedness matrix (GRM) using our SNP data was much more accurate, with relatedness estimates for mother-offspring pairs of on average 0.47 (expectation 0.5, min=0.42, max=0.52, see below for more detail). Therefore, we ran our quantitative genetics models using a GRM instead of a pedigree (Bérénos et al., 2014; Gervais et al., 2019). This has the added advantage that running these analyses with a GRM may improve the accuracy of quantitative genetics parameters given that a GRM should reflect the

realised proportion of genome pairs of individuals share (Gienapp et al., 2017).

To estimate a GRM, we first filtered the set of SNP loci to improve the precision and accuracy of the GRM, following Gervais et al. (2019), by further filtering SNPs for a MAF of at least 10%, resulting in a set of 1811 SNPs. While in some datasets, it has been suggested that more SNPs than this are required to accurately measure a GRM (Gervais et al., 2019), in others it has been found that only around 1000 loci are needed (Foroughirad et al., 2019). Furthermore, our accuracy in the GRM estimated from these data was good (see above); therefore, we believe our dataset to be large enough to accurately measure relatedness via a GRM. Prior to calculating the final GRM, we first used the filtered SNP set to identify and remove possible duplicate pairs of individuals contained in the dataset. Duplicate pairs of individuals may occur in cases where, for instance, an individual identification is lost (unreadable tattoo or failure to locate a microchip) on recapture, and they are treated as a new individual and given a new identification. Duplicate individuals were identified and removed from analyses using pairwise relatedness and confirmed via matched life-history data. To do this, we first identified pairs of sequenced samples that had extremely high estimated relatedness (threshold > 0.8) and were therefore likely duplicate samples of the same individual (Figure S1). This threshold was selected based on the upper tail of the total distribution of relatedness estimates, assuming that there should be a non-continuous distribution of relatedness values between (truly) highly related pairs and those that are instead duplicates. For each putative duplicated pair, we then cross-referenced with their estimated birth year and sex to ensure that they were indeed duplicates. This procedure identified 44 pairs of samples, and for each duplicated pair, the sample with the best quality genotyping data was kept. After removing duplicated individuals and re-filtering the SNP dataset according to parameters explained above, the final dataset for estimation of the GRM included 540 individuals and 1808 SNPs. Note that not all of these 540 individuals had phenotypic data for DFTD status associated with them, so therefore not all were included in the statistical analyses below. However, we retained all these individuals for the estimation of the GRM so as to improve precision of allele frequencies of the population required for estimating relatedness.

We next assessed which relatedness estimate performed best at estimating known relatives in this dataset ($N=51$ mother – pouch-young pairs in which both individuals had genetic data). Relatedness was estimated using six measures: *Yang* relatedness was estimated using GCTA (Yang et al., 2011), and *Wang*, *Queller and Goodnight*, *Dyad maximum likelihood*, *Lynch* and *Ritland* estimates were all estimated using *COANCESTRY* (Wang, 2010). Comparing pairwise relatedness estimates for all mother-offspring pairs (detailed above), the *Wang* relatedness estimate performed best, with an average relatedness for mother-offspring pairs of 0.47. We, therefore, used the GRM calculated using *Wang* relatedness estimate in all further quantitative genetic analyses. The variance in pairwise relatedness values using this estimate

was 0.007, with approximately 518 pairs of first-degree relatives (i.e., parent–offspring pairs or full siblings, $r > 0.45$) and 2414 pairs of second-degree relatives (e.g., half-siblings, $r = 0.2–0.3$) (out of a total of 145,530 possible pairs; [Figure S2](#)).

2.4 | Inbreeding coefficients

We measured variation in inbreeding using genomic inbreeding coefficients estimated in GCTA (Yang et al., 2011). We selected to use \hat{F}_{GRM} (hereafter F_{GRM}), which estimates the allelic correlation between gametes, as this measure has been found to be most closely correlated with runs of homozygosity on the genome (F_{ROH}), and is therefore likely a better measure of the genomic consequences of inbreeding (Yang et al., 2011). We ensured that F_{GRM} measures were robust to SNP filtering by varying the MAF cut-off criterion (1%, 5% and 10%). F_{GRM} estimates were all very highly correlated irrespective of which MAF cut-off we used ($r > 0.99\%$). Our genomic measure of inbreeding, F_{GRM} , ranged from -0.37 (indicating that the individual's parents are not related to each other) to 0.36 (indicating that the individual's parents are highly related to one another) (median $F_{\text{GRM}} = -0.04$, variance = 0.006 ; [Figure S3](#)).

2.5 | Statistical analyses

In all models, susceptibility to DFTD was fit as a case-control binary variable (1/0 case/control), where “cases” were captures of devils with a confirmed DFTD infection, and “controls” were captures of an uninfected individual. Note that we used a dataset containing repeated measures of all individuals, which in some cases means that an individual may first be considered a control before being diagnosed with DFTD at one or more subsequent recaptures. All models were fit in *stan* via the *brms* R package (Bürkner, 2017) using default flat priors on the fixed effects and half-Cauchy priors with two degrees of freedom on the random effects. All models were run for 10,000 iterations with a warm-up period of 2000 across four chains, and convergence was assessed by ensuring that R-hat was < 1.01 , effective sample sizes for all parameters were at least 1000 and by visually ensuring chains had mixed well. We report posterior medians for all parameters, which has been shown to be the least biased measure of central tendency of posterior distributions (Pick et al., 2023), together with a 95% credible interval (CI) of the posterior distributions. We consider there to be statistical evidence for a non-zero effect of fixed effects and covariance estimates when the 95% CI of the posterior distribution does not overlap zero. Variance estimates are bound to be positive given the half-Cauchy prior we used. Therefore, we considered there to be statistical evidence for variance components when the 95% CI of the posterior distribution for the proportion of phenotypic variance attributed to each random effect does not overlap 0.01.

2.5.1 | Selection on size via DFTD

We estimated the phenotypic relationship between susceptibility to DFTD and size traits by fitting a univariate mixed effects model of the effect of size traits on the probability of having DFTD, using the phenotypic dataset. Treating susceptibility to DFTD as a proxy for fitness, the regression coefficient of size on probability of having DFTD approximates selection on size traits caused by DFTD. This model (Model 1; [Table 1](#)) fits DFTD occurrence on a given capture with a logit link via the Bernoulli family and included the following fixed effects: *age in months* to account for increased likelihood of contracting the disease as devils age; *sex* to account for any potential sex differences in likelihood of contracting the disease; the interaction between *age* and *sex*; *year* as a covariate to account for the increase in disease presence in the population through time; *head width (mm)* and *body weight (kg)* measured at the same capture. We also fit as multi-level random effects: *year*, to account for repeated measures on multiple years and any non-linear variation between years in disease prevalence; *trap ID*, which described the location of the trap at which individuals were caught (trap locations were consistent across years) and was used to account for spatial environmental heterogeneity across the study area; and *individual ID* to account for repeated measures of individuals.

2.5.2 | Additive genetic variance (V_A) and inbreeding depression

To test whether there was evidence for variance in additive genetic effects (V_A) or inbreeding depression in any of the phenotypic traits (susceptibility to DFTD, head width, weight), we ran a suite of univariate animal models using the genetic dataset. Animal models extend linear mixed effects models by incorporating relatedness information to partition phenotypic variance into additive genetic and other sources of variance (Kruuk, 2004; Wilson et al., 2010). We ran a single model for each trait, where DFTD occurrence was fit with a logit link via the Bernoulli family (Model 2; [Table 1](#)), and head width and body weight were both fit as Gaussian traits (Models 3 and 4; [Table 1](#)).

Animal models were fit with the following fixed effects: *age in months* to account for growth and increased likelihood of contracting disease with age, *year* to account for phenotypic change through time, F_{GRM} to test for evidence for inbreeding depression, and the interaction between *age* and F_{GRM} to test whether the effect of inbreeding changed with age (Marjamäki et al., 2021). Animal models for head width and body weight further included *sex*, the quadratic effect of *age* (i.e., age^2) to account for non-linear growth curves, and the interaction between *sex* and *age*, and *sex* and age^2 . V_A was estimated in animal models by fitting the GRM as a covariance matrix. We estimated permanent environment effects variance (V_{PE}) by fitting repeated measures of individuals via a random effect for individual ID, which estimates among-individual variation in susceptibility to DFTD that is not caused by additive genetic effects and

TABLE 1 The structure of all linear mixed effects models outlined in *statistical analyses* section.

Model	Response	Fixed effects	Random effects	Family (link function)
<i>Univariate</i>				
1	DFTD	Age + Sex + Year + Head width + Body weight	Year + Trap + ID	Bernoulli (logit)
2	DFTD	Age + Year + F_{GRM} + Age: F_{GRM}	Year + Trap + ID + a	Bernoulli (logit)
3	Head width	Age + Age ² + Sex + Year + F_{GRM} + Age: F_{GRM} + Age:Sex + Age ² :Sex	Year + Trap + ID + a	Gaussian
4	Body weight	Age + Age ² + Sex + Year + F_{GRM} + Age: F_{GRM} + Age:Sex + Age ² :Sex	Year + Trap + ID + a	Gaussian
<i>Bivariate</i>				
5	Head width	Age + Age ² + Sex + Age:Sex + Age ² :Sex + F_{GRM}	Year + Trap + ID + a	Gaussian
	Body weight	Age + Age ² + Sex + Age:Sex + Age ² :Sex + F_{GRM}		Gaussian
6	Head width	Age + F_{GRM} + Year + Age ² + Sex + Age:Sex + Age ² :Sex	Year + Trap + ID + a	Gaussian
	DFTD	Age + F_{GRM} + Year		Bernoulli (logit)
7	Body weight	Age + F_{GRM} + Year + Age ² + Sex + Age:Sex + Age ² :Sex	Year + Trap + ID + a	Gaussian
	DFTD	Age + F_{GRM} + Year		Bernoulli (logit)

Note: All models were fit in stan via the brms package in R. *Model* refers to the model number referenced in text; *Response* refers to the response variable fit in the model; *Fixed effects* describes the fixed effects structure used in the model, where a colon represents an interaction term between two fixed effects; *Random effects* describes the random effects structure; *Family (link function)* describes the family with which the response variable was fit. Note that in bivariate models, the fixed effects structures varied between response variables and are shown on separate rows.

Abbreviations: a , additive genetic variance, estimated by fitting genomic relatedness matrix as a covariance matrix; Age, linear covariate describing age of individual in months; Age², the quadratic of age in months; Body weight, in kg; F_{GRM} , individuals inbreeding coefficient; Head width, in mm; ID, individual microchip; Sex, two-level effect "Male" or "Female"; Trap, the name of the location the observation was taken; Year, year of observation.

likely arise from environmental effects (both intrinsic and extrinsic to the individual). Animal models further included year as a random effect to account for non-linear variation across years (V_{Year}), as well as trap ID (V_{Trap}). Heritability (h^2) for each trait was then estimated as the proportion of phenotypic variance (measured as the sum of all variance components) explained by V_A . We also calculated the proportion of phenotypic variance attributed to V_{PE} , V_{Year} and V_{Trap} in the same way as for h^2 , which we refer to as the intra-class coefficient (ICC) for each term. We present estimates of heritability for DFTD on both the latent scale and observed data scale, which was estimated by converting latent-scale variance estimates to the data scale using the QGGLMM package in R (de Villemereuil et al., 2016). Latent scale heritability can be interpreted as the expected heritability for a hypothetical (latent) trait reflecting overall susceptibility to DFTD, whereas observed data-scale heritability can be interpreted as the heritability of the probability of being diagnosed with DFTD in the population, which incorporates sampling variance in the observed data. We present both of these estimates in the results as they may each be independently useful in predicting an evolutionary response in the probability that individuals will have DFTD or susceptibility to DFTD more generally, which may include multiple different traits.

Estimates of V_A can be inflated by maternal effects that are unaccounted for in our models (Kruuk & Hadfield, 2007; Wilson et al., 2005). Unfortunately, in these data, maternities for most individuals were unknown because pedigree reconstruction was not possible with the available SNP dataset (see above for details). However, we explored several alternative methods to quantify maternal effects to examine whether our estimates of V_A were being inflated by maternal effects (see Data S1). Estimates of V_A were not substantially inflated by not fitting maternal effects (estimated

inflation of $h^2 = 1\%$ for DFTD, 5% for weight and 3% for head width, see Data S1 and Figure S4), and thus, we present results without a maternal effects term fit.

Finally, to ensure that the temporal trends in either head width or body weight estimated in their respective models in this section did not arise as an artefact of using the genetic dataset, we ran models with head width and body weight as response variables using the phenotypic dataset that included the same fixed and random effects structure as the animal models (Models 3 and 4; Table 1), but without F_{GRM} or the relatedness matrix.

2.5.3 | Phenotypic, genetic and other covariances between traits

Phenotypic relationships may be causal if they are associated with a genetic covariance, but may also arise when some component of the environment is affecting each trait in parallel (Hajduk et al., 2018). As such, we next ran analyses to estimate the pairwise genetic covariances between susceptibility to DFTD and each of the two size traits. To do this, we ran a suite of bivariate animal models using the genetic dataset. These models used similar fixed and random effects structures to the univariate animal models explained in section *b*, but they were fit without year for head width and body weight and without the interaction between age and F for any trait because these effects were not different from zero (see results), and so we chose to remove these terms in order to simplify the models. All were fit with two response traits at a time in order to estimate variance-covariance matrices for each random effect (i.e., V_A , V_{PE} , V_{Year} , V_{Trap}). Specifically, we ran three bivariate models with the following combination

of response variables: (1) body weight and head width (Model 5; Table 1); (2) susceptibility to DFTD and head width (Model 6; Table 1) and (3) susceptibility to DFTD and body weight (Model 7; Table 1) (note that a single trivariate model of all three traits had convergence problems). Re-fitting bivariate models with a “body condition index” (i.e., body weight divided by head width) did not qualitatively change the results presented. Susceptibility to DFTD was fit as a binary variable with a logit link via the Bernoulli family, and head width and body weight were fit as Gaussian traits. As such, bivariate models including DFTD do not estimate a residual covariance between the binary and Gaussian trait (Bürkner, 2021). Therefore, we also fit bivariate models with “relative DFTD” fit with Gaussian errors, where relative DFTD was calculated by dividing observed DFTD at each observation by the mean probability of having DFTD. These models have the added advantage of directly estimating the selection differential between susceptibility to DFTD and size (see Price, 1970; Walsh & Lynch, 2018 for a detailed explanation). Although these models suggested that there was a negative residual covariance between susceptibility to DFTD and both body weight and head width, the overall qualitative inference of other covariance parameters did not change (Tables S3 and S5). We therefore present parameter estimates derived from models where DFTD was fit with a logit link. Furthermore, because phenotypic analyses in section *a* modelled size traits relative to each other, we re-fit the DFTD-head width and DFTD-body weight models (Table 1, Models 6 and 7) which fit the effect of weight on head width (Model 6) and the effect of head width on weight (Model 7). The qualitative inference from these models did not change overall, so we present results from models without these models without those additional effects fit (Table S4). All models estimated both covariances and correlations for each random effect, and we present both parameters. Note that while these models also estimated the variances estimated in univariate animal models fit in section *b*, we selected to report variance estimates from univariate models due to greater precision in variance estimates than estimated in bivariate models (i.e., narrower posterior distributions). Full variance-covariance matrices from bivariate models can be found in Table S5.

Finally, the phenotypic relationships estimated in section *a* were estimated from the phenotypic dataset which contained observations of individuals at least 14 months old for which there were complete phenotypic data ($N=1550$ recaptures of $N=729$ individuals). However, all quantitative genetic analyses used to estimate genetic variances and covariances were run with the genetic dataset which retained observations of individuals with genetic data ($N=498$ observations of $N=243$ individuals). Therefore, to ensure any differences in the phenotypic and genetic (or environmental) covariances were not artefacts that arose from the use of different datasets, we re-ran the phenotypic model described in section *a* with the genetic data to facilitate a more direct comparison with the estimated covariances.

TABLE 2 Results from a mixed effects model used to estimate phenotypic relationship between size traits (body weight and head width) and devil facial tumour disease (DFTD) occurrence.

Parameter	
<i>Fixed effects</i>	
Sex _M	-1.30 (-4.39 to 1.14)
Head width (mm)	0.32 (0.11 to 0.75)
Body weight (kg)	-0.83 (-2.18 to -0.09)
Age (months)	0.29 (0.10 to 0.83)
Year (continuous variable)	1.16 (0.48 to 3.02)
<i>Random effects</i>	
ID	7.31 (3.08 to 19.20)
Year	4.87 (1.89 to 12.85)
TrapD	1.87 (0.12 to 5.84)

Note: Response variable is the occurrence of DFTD at a given capture of an individual, fitted as a binary trait. *Trap* fitted the location of the trap where the individual was caught. Posterior medians of linear coefficient estimate for fixed effects and variance estimates for random effects are presented with 95% credible intervals of posterior distribution in parentheses. Fixed effect estimates where the 95% CIs do not overlap with zero are given in bold. Parameter estimates are on the logit link scale. The dataset used is the phenotypic data set with $N=729$ individuals over $N=1550$ captures, 22 years and 185 traps.

3 | RESULTS

3.1 | Selection on size via DFTD

There was no evidence for sex differences in the probability of having DFTD (Table 2). However, the probability of an individual having DFTD increased over the study period and also with individual age (Table 2). Devils with relatively larger heads had a greater probability of having DFTD, even after correcting for age (Table 2, Figure 1). Furthermore, devils with relatively lower body weight had a higher probability of having DFTD (Table 2 and Figure 1).

3.2 | Additive genetic variance (V_A) and inbreeding depression

In our animal models using the genetic dataset, we found effects of age and age² on both head width and body weight, indicating further growth in individuals older than 14 months old (see Table 3). There was also an effect of sex, reflecting sexual dimorphism in the species whereby adult males are larger than adult females (Table 3; average body weight: Males = 8.45 ± 2.02 kg, Females = 6.80 ± 1.48 kg), and an interaction between age and sex indicating greater rates of increase with age, even after 14 months. There was no evidence for any change over time in either head width or weight, as indicated by the 95% credible intervals for the linear effects of year overlapping zero (Table 3). Tests of temporal changes in either size trait using the

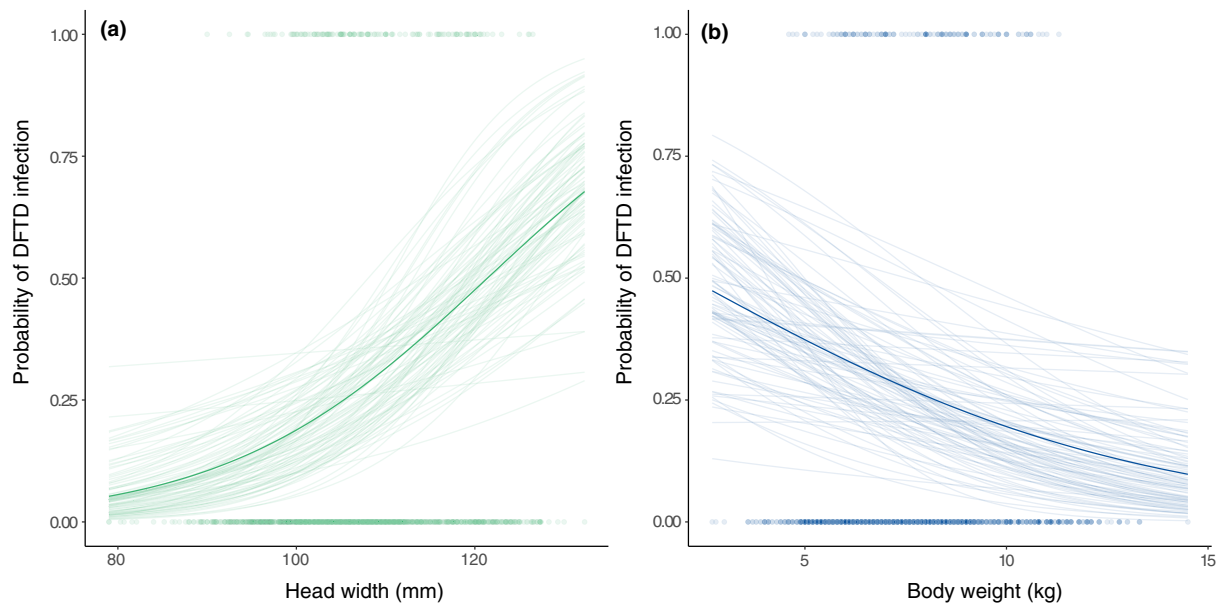


FIGURE 1 Plot showing the relationship between head width and devil facial tumour disease (DFTD) (a) and weight with DFTD (b). Points show observed data, and regression lines show the predicted relationship between size traits and DFTD derived from a mixed effects model which fits DFTD as a case-control response as a function of both size traits (see 2. Materials and methods for full model structure). Solid dark line shows predictions derived from the median of the posterior, and the lighter lines show 100 randomly selected draws from the posterior distribution.

larger phenotypic dataset yielded similar results, as both sets of analyses suggested that neither head width nor body weight was changing through time (see Table S2); these models also showed effectively the same sex and age effects as found in the genetic dataset.

Posterior distributions for estimates of additive genetic variance V_A from the animal models were different from zero for all three traits: the posterior probability of heritability being less than 0.01 (and therefore likely to be negligible) was <5% for all traits (i.e., 95% CI did not overlap 0.01, Table 3 and Figure 2). Heritability was estimated at 0.14 (95% CI=0.02–0.29) for head width and 0.23 for body weight (95% CI=0.09–0.38). Heritability for susceptibility to DFTD was estimated at 0.40 on the latent scale (95% CI=0.12–0.71) and 0.07 (95% CI=0.02–0.12) on the observed data scale (Figure 2). Head width and body weight showed quite high permanent environment effects variance (V_{PE}), but was almost twice as high for head width as for body weight (Figure 2). On the other hand, V_{PE} was very low for susceptibility to DFTD and the 5% CI for ICC_{PE} was lower than 0.01, suggesting that there may be negligible V_{PE} for susceptibility to DFTD (Figure 2 and Table 3). Phenotypic variation associated with among-year variation (V_{year}) was relatively high for all three traits (Figure 2 and Table 3). Phenotypic variation associated with spatial heterogeneity (measured via *Trap ID*) was very small for head width and susceptibility to DFTD, and the posterior probability for ICC_{Trap} being <0.01 was >5% for both traits, suggesting that V_{Trap} may account for very little phenotypic variance in these traits. On the other hand, V_{Trap} accounted for 38% phenotypic variance in body weight (95% CI=0.24–0.52) (Table 3 and Figure 2), suggesting that spatial heterogeneity may account for a large proportion of phenotypic variance in body weight.

There was no evidence for an effect of F_{GRM} on either head width, body weight or susceptibility to DFTD: the posterior distribution for the effect of F_{GRM} on all traits centred close to zero (Table 3), suggesting that there was no evidence of inbreeding depression in head width, body weight or susceptibility to DFTD. In identifying F_{GRM} for genotyped individuals, we found that there were approximately 8 individuals in the dataset that appeared very outbred (i.e., $F_{GRM} < -0.3$). This may arise as an artefact of the dataset (e.g., excess heterozygosity caused by sequencing error), but there was nothing in the data of these individuals that suggested that this was not a biological signal and this level of outbreeding may have emerged, for example, as a result of those individuals being immigrants to the study site. Nonetheless, removing these very outbred individuals did not change our inferences about inbreeding depression in this dataset.

3.3 | Phenotypic, genetic and other covariances between traits

3.3.1 | Head width and body weight

The total phenotypic covariance between head width and body weight, estimated as the sum of all covariances from the bivariate model, was positive ($COV_p=3.40$; 95% CI=2.45–4.47). The permanent environment effects covariance between head width and body weight was strongly positive (Table 4). There was no statistical support for a positive genetic covariance between head width and body weight as posterior distributions overlapped zero. The covariances for both other terms (year and trap) were not different from zero (Table 4).

TABLE 3 The results of animal models estimating V_A and the effect of FGRM on three traits: Head width, body weight and probability of having devil facial tumour disease (DFTD).

	Head width	Body weight	DFTD
Fixed effects			
Age	1.19 (0.96 to 1.42)	0.22 (0.16 to 0.28)	0.35 (0.12 to 0.75)
Age ²	-0.01 (-0.02 to -0.01)	-0.002 (-0.003 to -0.001)	-
Sex _M	-3.57 (-7.34 to 0.24)	-0.53 (-1.15 to 0.45)	-
F _{GRM}	-1.97 (-8.62 to 4.90)	-1.68 (-3.79 to 0.39)	-0.88 (-8.33 to 6.76)
Year	-0.17 (-0.43 to 0.09)	-0.01 (-0.06 to 0.04)	1.68 (0.63 to 3.49)
Age: Sex _M	0.57 (0.31 to 0.84)	0.12 (0.05 to 0.19)	-
Age ² : Sex _M	-0.01 (-0.02 to -0.01)	-0.002 (-0.003 to -0.002)	-
Random effects variance components			
V _A	4.74 (0.76 to 10.11)	0.36 (0.14 to 0.61)	34.83 (6.17 to 220.55)
V _{PE}	11.53 (6.92 to 16.96)	0.22 (0.03 to 0.45)	5.91 (0.05 to 60.41)
V _{Year}	7.08 (3.66 to 14.34)	0.21 (0.09 to 0.47)	39.03 (8.23 to 244.43)
V _{Trap}	0.25 (0.002 to 1.30)	0.15 (0.06 to 0.27)	1.89 (0.02 to 19.63)
V _R	9.25 (7.89 to 10.93)	0.56 (0.47 to 0.66)	-
Proportion of phenotypic variance			
h ²	0.14 (0.02 to 0.29)	0.23 (0.09 to 0.38)	0.40 (0.12 to 0.71)
ICC ^{PE}	0.34 (0.20 to 0.49)	0.15 (0.02 to 0.30)	0.07 (0.001 to 0.38)
ICC ^{Year}	0.21 (0.12 to 0.36)	0.14 (0.07 to 0.27)	0.44 (0.19 to 0.72)
ICC ^{Trap}	0.007 (0.0001 to 0.04)	0.38 (0.24 to 0.52)	0.02 (0.0002 to 0.13)

Note: Posterior medians of all effects are presented with 95% credible intervals of posterior distributions in parentheses. Fixed effect estimates where the 95% credible intervals of the posterior do not overlap with zero are in bold. Variance components and proportion of phenotypic variance for susceptibility to DFTD are shown on the latent (logit link) scale (estimates on the data scale can be found in Figure 2). Estimates where posterior distribution does not overlap with zero in bold. The dataset used has $N=243$ individuals over $N=498$ captures and 19 years and 128 traps. Linear coefficient estimates shown for fixed effects. Variance estimates shown for all random effects: variance in additive genetic effects (V_A); permanent environment effects (V_{PE}); year (V_{Year}); spatial location (V_{Trap}) and residual (V_R). Proportion of total phenotypic variance (i.e., sum of all variance components) attributed to additive genetic effects, also known as narrow-sense heritability (h^2); permanent environment effects (intra-class coefficient, ICC_{PE}); year (ICC_{Year}) and spatial location (ICC_{Trap}).

3.3.2 | DFTD and head width

There was no evidence for an overall phenotypic covariance between susceptibility to DFTD and head width, estimated as the sum of all covariances in a bivariate model using the genetic dataset ($COV_p=3.51$; 95% CI=-8.34-20.97). There was no statistical support for either a genetic or permanent environment covariance between the traits as the posterior distributions for both were wide and overlapped zero (Table 4 and Figure S5). Posterior distributions for both other terms (year and trap) also overlapped zero. The results are in contrast to the positive phenotypic association between susceptibility to DFTD and head width estimated from the phenotypic dataset in section a, which may have been because the phenotypic associations between size traits and susceptibility to DFTD were estimated as relative to each other (i.e., body weight relative to head width and vice versa). However, when we re-ran Model 1 (Table 1) with the genetic dataset, we again found no phenotypic association between susceptibility to DFTD and head width (see Table S1), suggesting instead that the contrasting conclusions concerning the association between DFTD

and head width likely occurred from differences between the two datasets.

3.3.3 | DFTD and body weight

We found that the total phenotypic covariance between susceptibility to DFTD and body weight, estimated as the sum of all covariances in a bivariate model, was negative ($COV_p=-2.69$; 95% CI=-7.77 to -0.71). The overall negative association was also confirmed when we re-ran the phenotypic selection model with the genetic dataset, where we found a negative phenotypic association between susceptibility to DFTD and body weight (see Table S1). We found a negative genetic covariance between the two traits, estimated at -2.56 (posterior median; 95% CI: -6.11 to -0.50). However, posterior distributions for the permanent environmental effects covariance between susceptibility to DFTD and body weight, as well as the covariances for the year and trap terms, were wide and overlapped zero (Table 4 and Figure S5). Although the

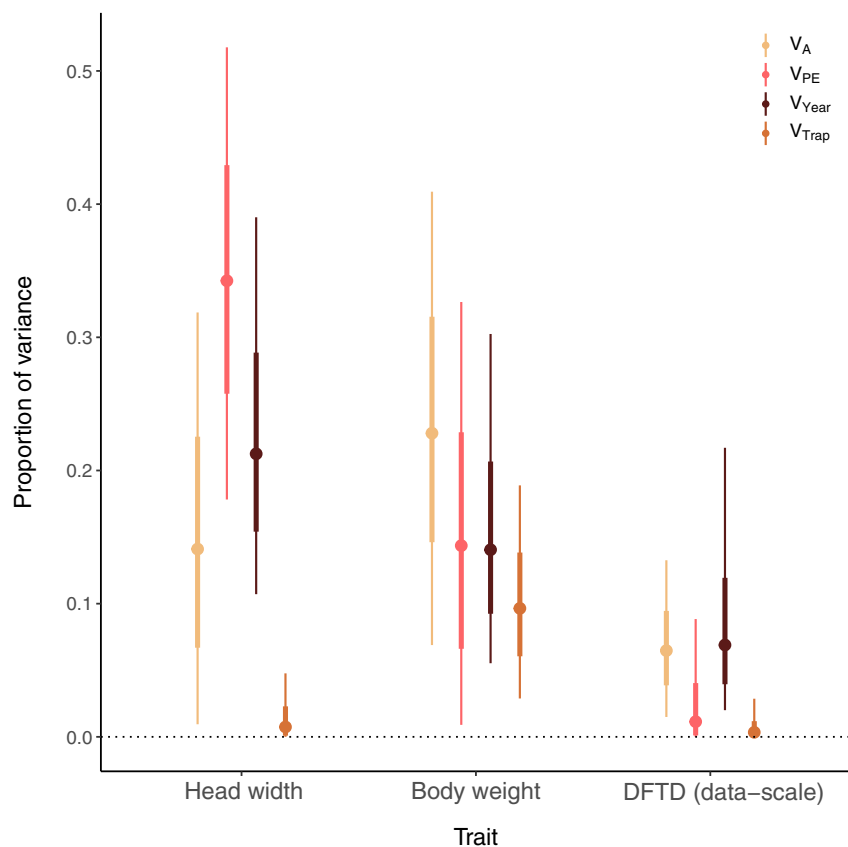


FIGURE 2 Plot showing proportion of phenotypic variance in devil facial tumour disease (DFTD), head width and weight attributed to variance in additive genetic effects (V_A) [reflecting narrow-sense heritability (h^2)]; permanent environment effects (V_{PE}); year (V_{Year}) and spatial location (V_{Trap}). Variances for DFTD shown on the observed data scale (see Table 2 for estimates on latent scale). Posterior median of estimates shown as point, with 75% CIs shown as heavy lines and 95% CIs as lighter line.

TABLE 4 The results of the three bivariate models used to estimate covariances between head width, body weight and devil facial tumour disease (DFTD).

	Head width and body weight	DFTD and head width	DFTD and body weight
COV_A	0.94 (-0.02 to 2.49)	-2.63 (-13.34 to 5.91)	-2.56 (-6.11 to -0.50)
COV_{PE}	2.03 (0.87 to 3.14)	0.26 (-5.40 to 6.18)	0.05 (-0.84 to 0.93)
COV_{Year}	-0.31 (-0.99 to 0.33)	6.78 (-2.18 to 21.16)	-1.06 (-3.43 to 0.53)
COV_{Trap}	0.02 (-0.08 to 0.17)	0.23 (-0.42 to 1.37)	0.29 (-0.12 to 1.02)
COV_{Res}	0.74 (0.47 to 1.04)	-	-
COV_P	3.40 (2.45 to 4.47)	3.51 (-8.34 to 20.97)	-2.69 (-7.77 to -0.71)

Note: Models were fit with DFTD as a binary variable with a logit link. Posterior medians of all covariance estimates presented with 95% credible intervals of posterior distribution in subscript parentheses. Covariances with DFTD given on the latent scale. Full variance-covariance matrices from models can be found in supplementary material (Table S4). Covariance estimates where posterior distribution does not overlap with zero in bold. The dataset used has $N=243$ individuals over $N=498$ captures and 19 years and 128 traps. Covariance estimates for additive genetic effects (COV_A), permanent environment effects (COV_{PE}), year effects (COV_{Year}), location effects (COV_{Trap}) and residual effects (COV_{Res}). Total phenotypic covariance between each pair of traits (COV_P) given as the sum of all covariances estimated from bivariate models.

credible interval for the genetic covariance was different from zero, posterior distributions for covariance estimates were all quite wide and uncertain.

4 | DISCUSSION

Our analyses of a long-term dataset of Tasmanian devils revealed evidence of additive genetic variance in susceptibility to DFTD, suggesting that there may be adaptive potential for Tasmanian devils to evolve resistance to DFTD, either directly via immune-related traits or via other traits (e.g., behaviour) that otherwise reduce individuals' exposure to the disease. There was no statistical evidence for inbreeding depression in susceptibility to DFTD, head width, or body weight. Finally, while there was evidence for a positive phenotypic relationship between head width and susceptibility to DFTD, this was not associated with a genetic covariance, whereas there was evidence that the negative phenotypic relationship between weight and susceptibility to DFTD was underpinned by a negative genetic covariance.

Additive genetic variance in a trait will determine the evolutionary response to selection on that trait (Golas et al., 2021; Walsh & Lynch, 2018). Our estimates of V_A confirm a genetic basis to susceptibility to DFTD in Tasmanian devils, which may result in the population evolving resistance to the disease. This result advances on a genome-wide association study which suggested that probability of having DFTD may have a genomic basis (Margres et al., 2018) and is also consistent with several previous studies indicating rapid evolutionary responses of devils as evidenced by allele frequency changes at some loci across the genome (Epstein et al., 2016; Fraik et al., 2020; Stahlke et al., 2021). Together with these previous studies, our results suggest that there may be some potential for the population to

respond adaptively to DFTD. In the absence of mutation and drift, strong directional selection on any fitness-related trait should eventually deplete additive genetic variance as alleles at causal loci move towards fixation (Bulmer, 1971). We may therefore expect that additive genetic variance in susceptibility to DFTD should decrease over time as the population evolves resistance. Alternatively, additive genetic variance may be maintained as a result of the continued evolution of DFTD, resulting in arms-race style host–pathogen coevolution (Best et al., 2008; Boots et al., 2009; Stammnitz et al., 2023). The realised evolutionary response in this population will therefore be the product of selection acting on both devils and DFTD, as well as the ecological environment in which devils live and are exposed to the disease. Additionally, it is highly likely that tolerance to DFTD is also evolving in the population (Hamede et al., 2020), which our analyses were not able to incorporate. Tolerance could be assessed from tracking disease progression and/or an individual's survival following infection. However, accurately measuring disease tolerance in mark-recapture studies can be inhibited by recapture probabilities, and although some work has been able to estimate population averages in tumour growth (Wells et al., 2017), future work could focus on incorporating individual-level data on tumour growth and survival post infection to investigate how disease tolerance evolves in populations facing EIDs.

Inbreeding depression occurs when recessive deleterious mutations are expressed as homozygotes as a result of inbreeding and negatively impact traits associated with fitness in a population (Charlesworth & Willis, 2009; DeRose & Roff, 1999). Interestingly, we did not find evidence for inbreeding depression in susceptibility to DFTD. Furthermore, while body weight has been found to be subject to inbreeding depression in many wild animals (Hajduk et al., 2018; Huisman et al., 2016; Laikre & Ryman, 1991; Nielsen et al., 2012), we did not find statistical support for inbreeding depression in body weight. Inbreeding depression in Tasmanian devils would be especially concerning considering the repeated historical population bottlenecks and recent steep declines in population size (Brüniche-Olsen et al., 2013, 2014; Lachish et al., 2007; Patton et al., 2020), and so the overall lack of evidence for inbreeding depression is positive when assessing the probability of the population's persistence. This is an interesting finding given that inbreeding depression has been found in other Tasmanian devil populations (Gooley et al., 2020), although studies of captive Tasmanian devils have also found a lack of inbreeding depression (Gooley et al., 2017). One explanation for the overall lack of inbreeding depression could be that recessive, deleterious alleles have already been purged from the population (Grossen et al., 2020; Hedrick & Garcia-Dorado, 2016; Kirkpatrick & Jarne, 2000) either via inbreeding or during the repeated population bottlenecks experienced across the species' range. Nonetheless, the expression of inbreeding depression may be dependent on both environmental conditions and genetic diversity within the population (Hedrick & Kalinowski, 2000), and while a lack of inbreeding depression provides a positive outlook for the

population now, it does not protect against inbreeding depression in the future.

Phenotypic and genetic covariances between DFTD and size traits can be used to predict whether either size trait will respond to selection caused by the disease (Price, 1970; Robertson & Lewontin, 1968) on the assumption that DFTD is a strong predictor of survival and/or reproduction and hence fitness. We found that weight and susceptibility to DFTD were phenotypically and genetically negatively correlated. It is important to note that our phenotypic analyses tested the effect of head width and body weight on DFTD concurrently, and therefore, our results reflect the effect of relative measures of each size trait. This means that we found that individuals with *relatively* greater body weight for a given head width (i.e., skeletal size) were less likely to have DFTD. The phenotypic covariance between these traits may reflect an immunocompetence – body condition relationship – whereby (relatively) heavier individuals are in better condition and consequently have better resistance to disease (Gleeson et al., 2005). Alternatively, the directionality of causality in the phenotypic covariance may be reversed whereby individuals that have the disease subsequently lose weight (Sánchez et al., 2018). As the observed negative phenotypic covariance was mirrored by a negative genetic covariance, this suggests that the relationship is more likely an indirect measure of body condition positively impacting immune function (Gleeson et al., 2005); however, further studies would be required to confirm the mechanistic relationship between the two traits.

We found that there was a positive phenotypic covariance between head width and susceptibility to DFTD at the phenotypic level, but we did not find evidence for this being underpinned by a genetic covariance. The underlying mechanisms causing the phenotypic relationship between susceptibility to DFTD and head width remain unclear, although one possibility is that the association may reflect an indirect association with social dominance. For instance, assuming that head width accurately predicts social dominance and males' access to mates in the breeding season when much of the transmission-relevant injurious biting occurs, the relationship between head width and susceptibility to DFTD may reflect a greater probability of infection caused by increased rates of the interactions that cause disease transmission that occur in socially dominant individuals (Hamede et al., 2008, 2009; Hamilton et al., 2019). Interestingly, we found that this relationship was not associated with a genetic covariance. However, re-running the phenotypic model with a smaller dataset did not indicate the same phenotypic relationship between susceptibility to DFTD and head width, suggesting that it is more likely that this dataset was limited in its statistical power to detect the phenotypic relationship, and therefore presumably also any associated genetic or environmental covariances.

In conclusion, EIDs are thought to dramatically alter the evolutionary dynamics of wild populations (Rogalski et al., 2017), but empirical evidence of this process is rare. We show that in an endangered marsupial facing an EID that has had a catastrophic impact

on the species, there is evolutionary potential in disease traits and current and ongoing selection acting on correlated morphological traits. Critically, we show that susceptibility to DFTD and size traits are all associated with underlying heritable genetic variance. We also show that these patterns exist in the absence of inbreeding depression. These results therefore not only provide important empirical evidence for how EIDs may shape future evolutionary dynamics of a population but also critically suggest that the species may hold the adaptive potential required to avoid extinction.

AUTHOR CONTRIBUTIONS

KS conceptualised, designed and led the research, analysed data and wrote the manuscript; MJ led the collection of field data and contributed to conceptual development; AS sequenced the samples; RH collected field data; PH sequenced the samples; MM sequenced the samples; HM collected field data and contributed to conceptual development; SC collected field data; SL collected field data; LK supervised the project and contributed critically to conceptualisation, statistical analyses and manuscript writing. All authors contributed to editing the manuscript and approved the final version.

ACKNOWLEDGEMENTS

We would like to first acknowledge the Toorono-maire-mener clan, the Traditional Custodians and First Peoples of the Freycinet Peninsula where this project was delivered, and we pay respect to their Elders past, present and emerging. We would also like to thank the many researchers involved in field sampling during the course of the study. We also thank Soraia Barbosa for facilitating the sharing of the genetic data and Alastair Wilson and an anonymous reviewer for constructive feedback on a previous version of this manuscript.

FUNDING INFORMATION

KS is funded by a European Research Council grant to LEBK; LEBK is funded by The Royal Society; genetic sequencing data were funded by the following grants awarded to AS and PH: NSF DEB-2027446, NIH R01-GM12653, NSF DEB-1316549; the long-term mark-recapture field study was supported by the following grants: Australian Research Council Discovery DP110102656, Australian Research Council Linkage Grant – LP0989613, Australian Research Council Linkage Grant – LP0561120, Australian Research Council Large Grant – A00000162, Australian Research Council Future Fellowship FT100100031 to MJ, Australian Research Council Australian Postdoctoral Fellowship to MJ.

CONFLICT OF INTEREST STATEMENT

The authors have no conflicts of interest to declare.

OPEN RESEARCH BADGES



This article has earned an Open Materials badge for making publicly available the components of the research methodology needed to

reproduce the reported procedure and analysis. All materials are available at https://github.com/kashastrickland/tasdevils_adaptivepotential.

DATA AVAILABILITY STATEMENT

All data required to reproduce results can be found at https://github.com/kashastrickland/tasdevils_adaptivepotential.

ORCID

Kasha Strickland <https://orcid.org/0000-0002-2490-0607>

Menna E. Jones <https://orcid.org/0000-0001-7558-9022>

Rodrigo K. Hamede <https://orcid.org/0000-0003-1526-225X>

Paul A. Hohenlohe <https://orcid.org/0000-0002-7616-0161>

Mark J. Margres <https://orcid.org/0000-0002-6153-6701>

Hamish I. McCallum <https://orcid.org/0000-0002-3493-0412>

Sebastien Comte <https://orcid.org/0000-0001-7984-8159>

Loeske E. B. Kruuk <https://orcid.org/0000-0001-8588-1123>

REFERENCES

- Ali, O. A., O'Rourke, S. M., Amish, S. J., Meek, M. H., Luikart, G., Jeffres, C., & Miller, M. R. (2016). RAD capture (rapture): Flexible and efficient sequence-based genotyping. *Genetics*, 202(2), 389–400. <https://doi.org/10.1534/genetics.115.183665>
- Altizer, S., Harvell, D., & Friedle, E. (2003). Rapid evolutionary dynamics and disease threats to biodiversity. *Trends in Ecology & Evolution*, 18(11), 589–596. <https://doi.org/10.1016/j.tree.2003.08.013>
- Bérénos, C., Ellis, P. A., Pilkington, J. G., & Pemberton, J. M. (2014). Estimating quantitative genetic parameters in wild populations: A comparison of pedigree and genomic approaches. *Molecular Ecology*, 23(14), 3434–3451. <https://doi.org/10.1111/mec.12827>
- Best, A., White, A., & Boots, M. (2008). Maintenance of host variation in tolerance to pathogens and parasites. *Proceedings of the National Academy of Sciences*, 105(52), 20786–20791. <https://doi.org/10.1073/pnas.0809558105>
- Bonneaud, C., Tardy, L., Giraudeau, M., Hill, G. E., McGraw, K. J., & Wilson, A. J. (2019). Evolution of both host resistance and tolerance to an emerging bacterial pathogen. *Evolution Letters*, 3(5), 544–554. <https://doi.org/10.1002/evl3.133>
- Boots, M., Best, A., Miller, M. R., & White, A. (2009). The role of ecological feedbacks in the evolution of host defence: What does theory tell us? *Philosophical Transactions of the Royal Society, B: Biological Sciences*, 364(1513), 27–36. <https://doi.org/10.1098/rstb.2008.0160>
- Brüniche-Olsen, A., Burrridge, C. P., Austin, J. J., & Jones, M. E. (2013). Disease induced changes in gene flow patterns among Tasmanian devil populations. *Biological Conservation*, 165, 69–78. <https://doi.org/10.1016/j.biocon.2013.05.014>
- Brüniche-Olsen, A., Jones, M. E., Austin, J. J., Burrridge, C. P., & Holland, B. R. (2014). Extensive population decline in the Tasmanian devil predates European settlement and devil facial tumour disease. *Biology Letters*, 10(11), 20140619. <https://doi.org/10.1098/rsbl.2014.0619>
- Bulmer, M. G. (1971). The effect of selection on genetic variability. *The American Naturalist*, 105(943), 201–211. <https://doi.org/10.1086/282718>
- Bürkner, P.-C. (2017). Brms: An R package for Bayesian multilevel models using Stan. *Journal of Statistical Software*, 80(1), 1–28.
- Bürkner, P.-C. (2021). Bayesian item response modeling in R with brms and Stan. *Journal of Statistical Software*, 100(5), 1–54. <https://doi.org/10.18637/jss.v100.i05>

- Catchen, J., Hohenlohe, P. A., Bassham, S., Amores, A., & Cresko, W. A. (2013). Stacks: An analysis tool set for population genomics. *Molecular Ecology*, 22(11), 3124–3140. <https://doi.org/10.1111/mec.12354>
- Charlesworth, D., & Willis, J. H. (2009). The genetics of inbreeding depression. *Nature Reviews Genetics*, 10(11), 783–796. <https://doi.org/10.1038/nrg2664>
- Coltman, D. W., Pilkington, J., Kruuk, L. E. B., Wilson, K., & Pemberton, J. M. (2001). Positive genetic correlation between parasite resistance and body size in a free-living ungulate population. *Evolution*, 55(10), 2116–2125. <https://doi.org/10.1111/j.0014-3820.2001.tb01326.x>
- Cristescu, R. H., Strickland, K., Schultz, A. J., Kruuk, L. E. B., de Villiers, D., & Frère, C. H. (2022). Susceptibility to a sexually transmitted disease in a wild koala population shows heritable genetic variance but no inbreeding depression. *Molecular Ecology*, 31(21), 5455–5467. <https://doi.org/10.1111/mec.16676>
- Cunningham, C. X., Comte, S., McCallum, H., Hamilton, D. G., Hamede, R., Storfer, A., Hollings, T., Ruiz-Aravena, M., Kerlin, D. H., Brook, B. W., Hocking, G., & Jones, M. E. (2021). Quantifying 25 years of disease-caused declines in Tasmanian devil populations: Host density drives spatial pathogen spread. *Ecology Letters*, 24(5), 958–969. <https://doi.org/10.1111/ele.13703>
- Daszak, P., Cunningham, A., & Hyatt, A. D. (2000). Emerging infectious diseases of wildlife—Threats to biodiversity and human health. *Science*, 287(5452), 443–449. <https://doi.org/10.1126/science.287.5452.443>
- de Villemereuil, P., Schielzeth, H., Nakagawa, S., & Morrissey, M. (2016). General methods for evolutionary quantitative genetic inference from generalized mixed models. *Genetics*, 204(3), 1281–1294. <https://doi.org/10.1534/genetics.115.186536>
- DeRose, M. A., & Roff, D. A. (1999). A comparison of inbreeding depression in LIFE-history and morphological traits in animals. *Evolution*, 53(4), 1288–1292. <https://doi.org/10.1111/j.1558-5646.1999.tb04541.x>
- Epstein, B., Jones, M., Hamede, R., Hendricks, S., McCallum, H., Murchison, E. P., Schönfeld, B., Wiench, C., Hohenlohe, P., & Storfer, A. (2016). Rapid evolutionary response to a transmissible cancer in Tasmanian devils. *Nature Communications*, 7(1), 12684. <https://doi.org/10.1038/ncomms12684>
- Fisher, M. C., & Garner, T. W. J. (2020). Chytrid fungi and global amphibian declines. *Nature Reviews Microbiology*, 18(6), 332–343. <https://doi.org/10.1038/s41579-020-0335-x>
- Foroughirad, V., Levensgood, A. L., Mann, J., & Frère, C. H. (2019). Quality and quantity of genetic relatedness data affect the analysis of social structure. *Molecular Ecology Resources*, 19, 1181–1194. <https://doi.org/10.1111/1755-0998.13028>
- Fraik, A. K., Margres, M. J., Epstein, B., Barbosa, S., Jones, M., Hendricks, S., Schönfeld, B., Stahlke, A. R., Veillet, A., Hamede, R., McCallum, H., Lopez-Contreras, E., Kallinen, S. J., Hohenlohe, P. A., Kelley, J. L., & Storfer, A. (2020). Disease swamps molecular signatures of genetic-environmental associations to abiotic factors in Tasmanian devil (*Sarcophilus harrisii*) populations. *Evolution*, 74(7), 1392–1408. <https://doi.org/10.1111/evo.14023>
- Gervais, L., Perrier, C., Bernard, M., Merlet, J., Pemberton, J. M., Pujol, B., & Quéméré, E. (2019). RAD-sequencing for estimating genomic relatedness matrix-based heritability in the wild: A case study in roe deer. *Molecular Ecology Resources*, 19(5), 1205–1217. <https://doi.org/10.1111/1755-0998.13031>
- Gienapp, P., Fior, S., Guillaume, F., Lasky, J. R., Sork, V. L., & Csilléry, K. (2017). Genomic quantitative genetics to study evolution in the wild. *Trends in Ecology & Evolution*, 32(12), 897–908. <https://doi.org/10.1016/j.tree.2017.09.004>
- Gleeson, D. J., Blows, M. W., & Owens, I. P. (2005). Genetic covariance between indices of body condition and immunocompetence in a passerine bird. *BMC Evolutionary Biology*, 5(1), 61. <https://doi.org/10.1186/1471-2148-5-61>
- Golas, B. D., Goodell, B., & Webb, C. T. (2021). Host adaptation to novel pathogen introduction: Predicting conditions that promote evolutionary rescue. *Ecology Letters*, 24(10), 2238–2255.
- Gooley, R. M., Hogg, C. J., Belov, K., & Grueber, C. E. (2017). No evidence of inbreeding depression in a Tasmanian devil insurance population despite significant variation in inbreeding. *Scientific Reports*, 7(1), 1830. <https://doi.org/10.1038/s41598-017-02000-y>
- Gooley, R. M., Hogg, C. J., Fox, S., Pemberton, D., Belov, K., & Grueber, C. E. (2020). Inbreeding depression in one of the last DFTD-free wild populations of Tasmanian devils. *PeerJ*, 8, e9220. <https://doi.org/10.7717/peerj.9220>
- Grossen, C., Guillaume, F., Keller, L. F., & Croll, D. (2020). Purging of highly deleterious mutations through severe bottlenecks in alpine ibex. *Nature Communications*, 11(1), 1001. <https://doi.org/10.1038/s41467-020-14803-1>
- Hajduk, G. K., Cockburn, A., Margraf, N., Osmond, H. L., Walling, C. A., & Kruuk, L. E. B. (2018). Inbreeding, inbreeding depression, and infidelity in a cooperatively breeding bird. *Evolution*, 72(7), 1500–1514. <https://doi.org/10.1111/evo.13496>
- Hamede, R. K., Bashford, J., McCallum, H., & Jones, M. (2009). Contact networks in a wild Tasmanian devil (*Sarcophilus harrisii*) population: Using social network analysis to reveal seasonal variability in social behaviour and its implications for transmission of devil facial tumour disease. *Ecology Letters*, 12(11), 1147–1157. <https://doi.org/10.1111/j.1461-0248.2009.01370.x>
- Hamede, R. K., McCallum, H., & Jones, M. (2008). Seasonal, demographic and density-related patterns of contact between Tasmanian devils (*Sarcophilus harrisii*): Implications for transmission of devil facial tumour disease. *Austral Ecology*, 33(5), 614–622. <https://doi.org/10.1111/j.1442-9993.2007.01827.x>
- Hamede, R. K., McCallum, H., & Jones, M. (2013). Biting injuries and transmission of Tasmanian devil facial tumour disease. *Journal of Animal Ecology*, 82(1), 182–190. <https://doi.org/10.1111/j.1365-2656.2012.02025.x>
- Hamede, R. K., Owen, R., Siddle, H., Peck, S., Jones, M., Dujon, A. M., Giraudeau, M., Roche, B., Ujvari, B., & Thomas, F. (2020). The ecology and evolution of wildlife cancers: Applications for management and conservation. *Evolutionary Applications*, 13(7), 1719–1732. <https://doi.org/10.1111/eva.12948>
- Hamede, R. K., Pearce, A.-M., Swift, K., Barmuta, L. A., Murchison, E. P., & Jones, M. E. (2015). Transmissible cancer in Tasmanian devils: Localized lineage replacement and host population response. *Proceedings of the Royal Society B: Biological Sciences*, 282(1814), 20151468. <https://doi.org/10.1098/rspb.2015.1468>
- Hamilton, D. G., Jones, M. E., Cameron, E. Z., Kerlin, D. H., McCallum, H., Storfer, A., Hohenlohe, P. A., & Hamede, R. K. (2020). Infectious disease and sickness behaviour: Tumour progression affects interaction patterns and social network structure in wild Tasmanian devils. *Proceedings of the Royal Society B: Biological Sciences*, 287, 20202454. <https://doi.org/10.1098/rspb.2020.2454>
- Hamilton, D. G., Jones, M. E., Cameron, E. Z., McCallum, H., Storfer, A., Hohenlohe, P. A., & Hamede, R. K. (2019). Rate of intersexual interactions affects injury likelihood in Tasmanian devil contact networks. *Behavioral Ecology*, 30(4), 1087–1095. <https://doi.org/10.1093/beheco/arz054>
- Hawkins, C. E., Baars, C., Hesterman, H., Hocking, G. J., Jones, M. E., Lazenby, B., Mann, D., Mooney, N., Pemberton, D., Pyecroft, S., Restani, M., & Wiersma, J. (2006). Emerging disease and population decline of an Island endemic, the Tasmanian devil *Sarcophilus harrisii*. *Infectious Disease and Mammalian Conservation*, 131(2), 307–324. <https://doi.org/10.1016/j.biocon.2006.04.010>
- Hayward, A. D., Nussey, D. H., Wilson, A. J., Berenos, C., Pilkington, J. G., Watt, K. A., Pemberton, J. M., & Graham, A. L. (2014). Natural selection on individual variation in tolerance of gastrointestinal nematode infection. *PLoS Biology*, 12(7), e1001917. <https://doi.org/10.1371/journal.pbio.1001917>

- Healy, K., Ezard, T. H. G., Jones, O. R., Salguero-Gómez, R., & Buckley, Y. M. (2019). Animal life history is shaped by the pace of life and the distribution of age-specific mortality and reproduction. *Nature Ecology & Evolution*, 3(8), 1217–1224. <https://doi.org/10.1038/s41559-019-0938-7>
- Hedrick, P. W., & Garcia-Dorado, A. (2016). Understanding inbreeding depression, purging, and genetic rescue. *Trends in Ecology & Evolution*, 31(12), 940–952. <https://doi.org/10.1016/j.tree.2016.09.005>
- Hedrick, P. W., & Kalinowski, S. T. (2000). Inbreeding depression in conservation biology. *Annual Review of Ecology and Systematics*, 31(1), 139–162. <https://doi.org/10.1146/annurev.ecolsys.31.1.139>
- Herrera, J., & Nunn, C. L. (2019). Behavioural ecology and infectious disease: Implications for conservation of biodiversity. *Philosophical Transactions of the Royal Society, B: Biological Sciences*, 374(1781), 20180054. <https://doi.org/10.1098/rstb.2018.0054>
- Hoffmann, A. A., Sgrò, C. M., & Kristensen, T. N. (2017). Revisiting adaptive potential, population size, and conservation. *Trends in Ecology & Evolution*, 32(7), 506–517. <https://doi.org/10.1016/j.tree.2017.03.012>
- Hoffmann, C., Zimmermann, F., Biek, R., Kuehl, H., Nowak, K., Mundry, R., Agbor, A., Angedakin, S., Arandjelovic, M., Blankenburg, A., Brazolla, G., Corogenes, K., Couacy-Hymann, E., Deschner, T., Diegues, P., Dierks, K., Düx, A., Dupke, S., Eshuis, H., ... Leendertz, F. H. (2017). Persistent anthrax as a major driver of wildlife mortality in a tropical rainforest. *Nature*, 548(7665), 82–86. <https://doi.org/10.1038/nature23309>
- Hoyt, J. R., Kilpatrick, A. M., & Langwig, K. E. (2021). Ecology and impacts of white-nose syndrome on bats. *Nature Reviews Microbiology*, 19(3), 196–210. <https://doi.org/10.1038/s41579-020-00493-5>
- Huisman, J., Kruuk, L. E. B., Ellis, P. A., Clutton-Brock, T., & Pemberton, J. M. (2016). Inbreeding depression across the lifespan in a wild mammal population. *Proceedings of the National Academy of Sciences*, 113(13), 3585–3590. <https://doi.org/10.1073/pnas.1518046113>
- Jones, M. E. (2023). Over-eruption in marsupial carnivore teeth: Compensation for a constraint. *Proceedings of the Royal Society B: Biological Sciences*, 290, 20230644. <https://doi.org/10.1098/rspb.2023.0644>
- Jones, M. E., Cockburn, A., Hamede, R., Hawkins, C., Hesterman, H., Lachish, S., Mann, D., McCallum, H., & Pemberton, D. (2008). Life-history change in disease-ravaged Tasmanian devil populations. *Proceedings of the National Academy of Sciences*, 105(29), 10023–10027. <https://doi.org/10.1073/pnas.0711236105>
- Kirkpatrick, M., & Jarne, P. (2000). The effects of a bottleneck on inbreeding depression and the genetic load. *The American Naturalist*, 155(2), 154–167. <https://doi.org/10.1086/303312>
- Kruuk, L. E. B. (2004). Estimating genetic parameters in natural populations using the 'animal model'. *Proceedings of the Royal Society of London. Series B*, 359, 873–890.
- Kruuk, L. E. B., & Hadfield, J. D. (2007). How to separate genetic and environmental causes of similarity between relatives. *Journal of Evolutionary Biology*, 20(5), 1890–1903. <https://doi.org/10.1111/j.1420-9101.2007.01377.x>
- Lachish, S., Jones, M., & McCallum, H. (2007). The impact of disease on the survival and population growth rate of the Tasmanian devil. *Journal of Animal Ecology*, 76(5), 926–936.
- Lachish, S., McCallum, H., & Jones, M. (2009). Demography, disease and the devil: Life-history changes in a disease-affected population of Tasmanian devils (*Sarcophilus harrisii*). *Journal of Animal Ecology*, 78(2), 427–436.
- Laikre, L., & Ryman, N. (1991). Inbreeding depression in a captive wolf (*Canis lupus*) population. *Conservation Biology*, 5(1), 33–40. <https://doi.org/10.1111/j.1523-1739.1991.tb00385.x>
- Margres, M. J., Jones, M. E., Epstein, B., Kerlin, D. H., Comte, S., Fox, S., Fraik, A. K., Hendricks, S. A., Huxtable, S., Lachish, S., Lazenby, B., O'Rourke, S. M., Stahlke, A. R., Wiench, C. G., Hamede, R., Schönfeld, B., McCallum, H., Miller, M. R., Hohenlohe, P. A., & Storfer, A. (2018). Large-effect loci affect survival in Tasmanian devils (*Sarcophilus harrisii*) infected with a transmissible cancer. *Molecular Ecology*, 27(21), 4189–4199. <https://doi.org/10.1111/mec.14853>
- Marjamäki, P. H., Dugdale, H. L., Delahay, R., McDonald, R. A., & Wilson, A. J. (2021). Genetic, social and maternal contributions to *Mycobacterium bovis* infection status in European badgers (*Meles meles*). *Journal of Evolutionary Biology*, 34(4), 695–709.
- Martin, A. M., Cassirer, E. F., Waits, L. P., Plowright, R. K., Cross, P. C., & Andrews, K. R. (2021). Genomic association with pathogen carriage in bighorn sheep (*Ovis canadensis*). *Ecology and Evolution*, 11(6), 2488–2502.
- McCallum, H. (2008). Tasmanian devil facial tumour disease: Lessons for conservation biology. *Trends in Ecology & Evolution*, 23(11), 631–637. <https://doi.org/10.1016/j.tree.2008.07.001>
- McCallum, H., Tompkins, D. M., Jones, M., Lachish, S., Marvanek, S., Lazenby, B., Hocking, G., Wiersma, J., & Hawkins, C. E. (2007). Distribution and impacts of Tasmanian devil facial tumor disease. *EcoHealth*, 4(3), 318–325. <https://doi.org/10.1007/s10393-007-0118-0>
- Medzhitov, R., Schneider, D. S., & Soares, M. P. (2012). Disease tolerance as a defense strategy. *Science*, 335(6071), 936–941. <https://doi.org/10.1126/science.1214935>
- Murchison, E. P., Schulz-Trieglaff, O. B., Ning, Z., Alexandrov, L. B., Bauer, M. J., Fu, B., Hims, M., Ding, Z., Ivakhno, S., Stewart, C., Ng, B. L., Wong, W., Aken, B., White, S., Alsop, A., Becq, J., Bignell, G. R., Cheetham, R. K., Cheng, W., & Stratton, M. R. (2012). Genome sequencing and analysis of the Tasmanian devil and its transmissible cancer. *Cell*, 148(4), 780–791. <https://doi.org/10.1016/j.cell.2011.11.065>
- Murchison, E. P., Tovar, C., Hsu, A., Bender, H. S., Kheradpour, P., Rebbeck, C. A., Obendorf, D., Conlan, C., Bahlo, M., Blizzard, C. A., Pyecroft, S., Kreiss, A., Kellis, M., Stark, A., Harkins, T. T., Graves, J. A. M., Woods, G. M., Hannon, G. J., & Papenfuss, A. T. (2010). The Tasmanian devil transcriptome Reveals Schwann cell origins of a clonally transmissible cancer. *Science*, 327(5961), 84–87. <https://doi.org/10.1126/science.1180616>
- Nielsen, J. F., English, S., Goodall-Copestake, W. P., Wang, J., Walling, C. A., Bateman, A. W., Flower, T. P., Sutcliffe, R. L., Samson, J., Thavarajah, N. K., Kruuk, L. E. B., Clutton-Brock, T. H., & Pemberton, J. M. (2012). Inbreeding and inbreeding depression of early life traits in a cooperative mammal. *Molecular Ecology*, 21(11), 2788–2804. <https://doi.org/10.1111/j.1365-294X.2012.05565.x>
- O'Grady, J. J., Brook, B. W., Reed, D. H., Ballou, J. D., Tonkyn, D. W., & Frankham, R. (2006). Realistic levels of inbreeding depression strongly affect extinction risk in wild populations. *Biological Conservation*, 133(1), 42–51. <https://doi.org/10.1016/j.biocon.2006.05.016>
- Patton, A. H., Lawrance, M. F., Margres, M. J., Kozakiewicz, C. P., Hamede, R., Ruiz-Aravena, M., Hamilton, D. G., Comte, S., Ricci, L. E., Taylor, R. L., Stadler, T., Leaché, A., McCallum, H., Jones, M. E., Hohenlohe, P. A., & Storfer, A. (2020). A transmissible cancer shifts from emergence to endemism in Tasmanian devils. *Science*, 370(6522), eabb9772. <https://doi.org/10.1126/science.abb9772>
- Pick, J. L., Kasper, C., Allegue, H., Dingemans, N. J., Dochtermann, N. A., Laskowski, K. L., Lima, M. R., Schielzeth, H., Westneat, D. F., Wright, J., & Araya-Ajoy, Y. G. (2023). Describing posterior distributions of variance components: Problems and the use of null distributions to aid interpretation. *Methods in Ecology and Evolution*, 14(10), 2557–2574. <https://doi.org/10.1111/2041-210X.14200>
- Price, G. R. (1970). Selection and covariance. *Nature*, 227, 520–521. <https://doi.org/10.1038/227520a0>
- Pye, R., Hamede, R., Siddle, H. V., Caldwell, A., Knowles, G. W., Swift, K., Kreiss, A., Jones, M. E., Lyons, A. B., & Woods, G. M. (2016).

- Demonstration of immune responses against devil facial tumour disease in wild Tasmanian devils. *Biology Letters*, 12(10), 20160553. <https://doi.org/10.1098/rsbl.2016.0553>
- Rarberg, L., & Stjernman, M. (2003). Natural selection on immune responsiveness in blue tits *Parus caeruleus*. *Evolution*, 57(7), 1670–1678. <https://doi.org/10.1111/j.0014-3820.2003.tb00372.x>
- Reid, J. M., Arcese, P., & Keller, L. F. (2003). Inbreeding depresses immune response in song sparrows (*Melospiza melodia*): Direct and inter-generational effects. *Proceedings of the Royal Society of London, Series B: Biological Sciences*, 270(1529), 2151–2157. <https://doi.org/10.1098/rspb.2003.2480>
- Rigby, M. C., Hechinger, R. F., & Stevens, L. (2002). Why should parasite resistance be costly? *Trends in Parasitology*, 18(3), 116–120. [https://doi.org/10.1016/S1471-4922\(01\)02203-6](https://doi.org/10.1016/S1471-4922(01)02203-6)
- Robertson, A., & Lewontin, R. (1968). *Population biology and evolution. The spectrum of genetic variation* (pp. 5–16). Syracuse University Press.
- Rogalski, M. A., Gowler, C. D., Shaw, C. L., Hufbauer, R. A., & Duffy, M. A. (2017). Human drivers of ecological and evolutionary dynamics in emerging and disappearing infectious disease systems. *Philosophical Transactions of the Royal Society, B: Biological Sciences*, 372(1712), 20160043. <https://doi.org/10.1098/rstb.2016.0043>
- Ross-Gillespie, A., O'Riain, M. J., & Keller, L. F. (2007). Viral epizootic reveals inbreeding depression in a habitually inbreeding mammal. *Evolution*, 61(9), 2268–2273. <https://doi.org/10.1111/j.1558-5646.2007.00177.x>
- Sánchez, C. A., Becker, D. J., Teitelbaum, C. S., Barriga, P., Brown, L. M., Majewska, A. A., Hall, R. J., & Altizer, S. (2018). On the relationship between body condition and parasite infection in wildlife: A review and meta-analysis. *Ecology Letters*, 21(12), 1869–1884. <https://doi.org/10.1111/ele.13160>
- Schrag, S. J., & Wiener, P. (1995). Emerging infectious disease: What are the relative roles of ecology and evolution? *Trends in Ecology & Evolution*, 10(8), 319–324. [https://doi.org/10.1016/S0169-5347\(00\)89118-1](https://doi.org/10.1016/S0169-5347(00)89118-1)
- Silk, M. J., & Hodgson, D. J. (2021). Life history and population regulation shape demographic competence and influence the maintenance of endemic disease. *Nature Ecology & Evolution*, 5(1), 82–91. <https://doi.org/10.1038/s41559-020-01333-8>
- Spielman, D., Brook, B. W., Briscoe, D. A., & Frankham, R. (2004). Does inbreeding and loss of genetic diversity decrease disease resistance? *Conservation Genetics*, 5(4), 439–448. <https://doi.org/10.1023/B:COGE.0000041030.76598.cd>
- Stahlke, A. R., Epstein, B., Barbosa, S., Margres, M. J., Patton, A. H., Hendricks, S. A., Veillet, A., Fraik, A. K., Schönfeld, B., McCallum, H. I., Hamede, R., Jones, M. E., Storfer, A., & Hohenlohe, P. A. (2021). Contemporary and historical selection in Tasmanian devils (*Sarcophilus harrisii*) support novel, polygenic response to transmissible cancer. *Proceedings of the Royal Society B: Biological Sciences*, 288, 20210577. <https://doi.org/10.1098/rspb.2021.0577>
- Stammnitz, M. R., Gori, K., Kwon, Y. M., Harry, E., Martin, F. J., Billis, K., Cheng, Y., Baez-Ortega, A., Chow, W., Comte, S., Eggertsson, H., Fox, S., Hamede, R., Jones, M., Lazenby, B., Peck, S., Pye, R., Quail, M. A., Swift, K., & Murchison, E. P. (2023). The evolution of two transmissible cancers in Tasmanian devils. *Science*, 380(6642), 283–293. <https://doi.org/10.1126/science.abq6453>
- Trinkel, M., Cooper, D., Packer, C., & Slotow, R. (2011). Inbreeding depression increases susceptibility to bovine tuberculosis in lions: An experimental test using an inbred–outbred contrast through translocation. *Journal of Wildlife Diseases*, 47(3), 494–500. <https://doi.org/10.7589/0090-3558-47.3.494>
- Valenzuela-Sánchez, A., Wilber, M. Q., Canessa, S., Bacigalupe, L. D., Muths, E., Schmidt, B. R., Cunningham, A. A., Ozgul, A., Johnson, P. T. J., & Cayuela, H. (2021). Why disease ecology needs life-history theory: A host perspective. *Ecology Letters*, 24(4), 876–890. <https://doi.org/10.1111/ele.13681>
- Walsh, B., & Lynch, M. (2018). *Evolution and selection of quantitative traits*. Oxford University Press.
- Wang, J. (2010). Coancestry: A program for simulating, estimating and analysing relatedness and inbreeding coefficients. *Molecular Ecology Resources*, 11(1), 141–145. <https://doi.org/10.1111/j.1755-0998.2010.02885.x>
- Wells, K., Hamede, R. K., Kerlin, D. H., Storfer, A., Hohenlohe, P. A., Jones, M. E., & McCallum, H. I. (2017). Infection of the fittest: Devil facial tumour disease has greatest effect on individuals with highest reproductive output. *Ecology Letters*, 20(6), 770–778. <https://doi.org/10.1111/ele.12776>
- Wilson, A. J., Coltman, D. W., Pemberton, J. M., Overall, A. D. J., Byrne, K. A., & Kruuk, L. E. B. (2005). Maternal genetic effects set the potential for evolution in a free-living vertebrate population. *Journal of Evolutionary Biology*, 18(2), 405–414. <https://doi.org/10.1111/j.1420-9101.2004.00824.x>
- Wilson, A. J., Réale, D., Clements, M. N., Morrissey, M. M., Postma, E., Walling, C. A., Kruuk, L. E. B., & Nussey, D. H. (2010). An ecologist's guide to the animal model. *Journal of Animal Ecology*, 79(1), 13–26. <https://doi.org/10.1111/j.1365-2656.2009.01639.x>
- Yang, J., Lee, S. H., Goddard, M. E., & Visscher, P. M. (2011). GCTA: A tool for genome-wide complex trait analysis. *American Journal of Human Genetics*, 88(1), 76–82. <https://doi.org/10.1016/j.ajhg.2010.11.011>

SUPPORTING INFORMATION

Additional supporting information can be found online in the Supporting Information section at the end of this article.

How to cite this article: Strickland, K., Jones, M. E., Storfer, A., Hamede, R. K., Hohenlohe, P. A., Margres, M. J., McCallum, H. I., Comte, S., Lachish, S., & Kruuk, L. E. B. (2024). Adaptive potential in the face of a transmissible cancer in Tasmanian devils. *Molecular Ecology*, 00, e17531. <https://doi.org/10.1111/mec.17531>